Non-covalent biofunctionalization of single-walled carbon nanotubes *via* biotin attachment by π-stacking interactions and pyrrole polymerization

R. Haddad,[ab] S. Cosnier,*[a] A. Maaref[b] and M. Holzinger[a]

Received 13th August 2009, Accepted 22nd September 2009
First published as an Advance Article on the web 29th September 2009
DOI: 10.1039/b916774a

Single-walled carbon nanotubes were functionalized with biotin using either electropolymerization or formation of π-stacking interactions for the construction of biosensors. Thanks to the high affinity of the avidin–biotin interactions, a biotinylated glucose oxidase (B-GOX) as a biomolecule model was immobilized on the biotinylated nanotubes. The influence of the biosensor configuration on their amperometric performances was investigated by changing the amount of nanotubes and the numbers of avidin/B-GOX layers. By increasing the amount of nanotube and avidin/B-GOX layers, both sensor setups show a perfect linear increase of immobilized enzymes reflecting a high reproducibility of our systems. The highest sensitivities (up to 5.2 mA M^{-1} cm^{-2}) and maximum current densities (up to 55 μA cm^{-2}) were obtained using nanotube deposits modified by electrochemical coatings. In contrast, non-covalently functionalized biotin-nanotubes show a better permeability for the enzymatically generated hydrogen peroxide.

1. Introduction

During the last 20 years, a revolution appeared in sensor research, giving birth to a large number of sensor devices for medical[1,2] and environmental technology.[3,4] Investment and development in this field expanded exponentially. In particular, glucose biosensors received enormous attention due to the need of new developments for the diagnosis and control of diabetes.[5–7] Moreover, electrochemical biosensors based on the use of enzymes, antibodies or antigens have received considerable attention due to the advantages of the association of the high specific recognition properties of biomolecules with the sensitivity and versatility of the amperometric, potentiometric or impedimetric transduction.

However, one of the limitations of common biosensors resides in the amount of active biomolecule immobilized per surface unit. The sensitivity of the molecular recognition event (enzymatic reaction, immunoreaction and even hybridization) indeed is mainly proportional to the electrode surface. The concept of biomolecule immobilization by affinity interactions should preserve the biological activity by formation of a single attachment point enabling a specific orientation. The principal approach consists of the immobilization of biotinylated biomolecules on biotin covered surfaces *via* avidin bridges between the two biotinylated components. The strong associations between biotin (a vitamin) and avidin (a protein with four biotin specific cavities) were widely used for ELISA assays. The electrogeneration of biotinylated polymer films enabled therefore the successive attachment of avidin and biotinylated proteins, oligonucleotides or bacteria on the transducer surface

Significant efforts focalize on the development of three-dimensional biomaterials to improve the detection limit. Among the various possibilities envisioned for such goals, the use of carbon nanotubes (CNTs) aroused an increasing interest owing to the geometry and conductivity of this material. Nanotubes have an impressive high specific surface of around 1000 m^2 g^{-1}, making them promising candidates for the construction of highly porous three-dimensional nanostructured frameworks. Moreover, the high conductivity of CNTs may be utilized to extend the electrochemical transduction step localized at the electrode surface to the whole three-dimensional structure of biocoatings based on CNT scaffolds. However, the biomolecule immobilization on CNT deposits was mainly performed by entrapment within a matrix,[8,9] spread or generated onto CNT coatings preventing thus direct electrical communication between biomolecule and CNT.[10,11]

To circumvent this drawback, biomolecule immobilization was carried out by its direct covalent binding onto the CNT surface.[12] However, this approach requires, first, the chemical modification of CNTs (for instance, their chemical oxidation for creating carboxylic groups) that drastically reduces their electronic conductivity.

In this context, we report here the original non-covalent modification of single-walled carbon nanotubes (SWCNTs) by biotin groups allowing the immobilization of biotinylated biomolecules in the close proximity of carbon nanotube surface by affinity interactions *via* the avidin–biotin system. The SWCNT modification by biotin was achieved *via* π-stacking interactions between the nanotube sidewall and a biotinylated pyrene derivative (Scheme 1A) or by electropolymerization of a biotin derivative functionalized by a pyrrole group (Scheme 1B). The resulting biotinylated SWCNT coatings were used for the successive attachment of avidin and biotin-labelled glucose oxidase chosen as the biomolecule model. The efficiency of the biomolecule anchoring was investigated by fluorescence

[a]*Département de Chimie Moléculaire, UMR-5250, ICMG FR-2607, CNRS, Université Joseph Fourier BP 53, 38041 Grenoble Cédex 9, France*
[b]*Laboratoire de Physique et Chimie des Interfaces, Faculté des Sciences-Monastir 5000, Tunisia*

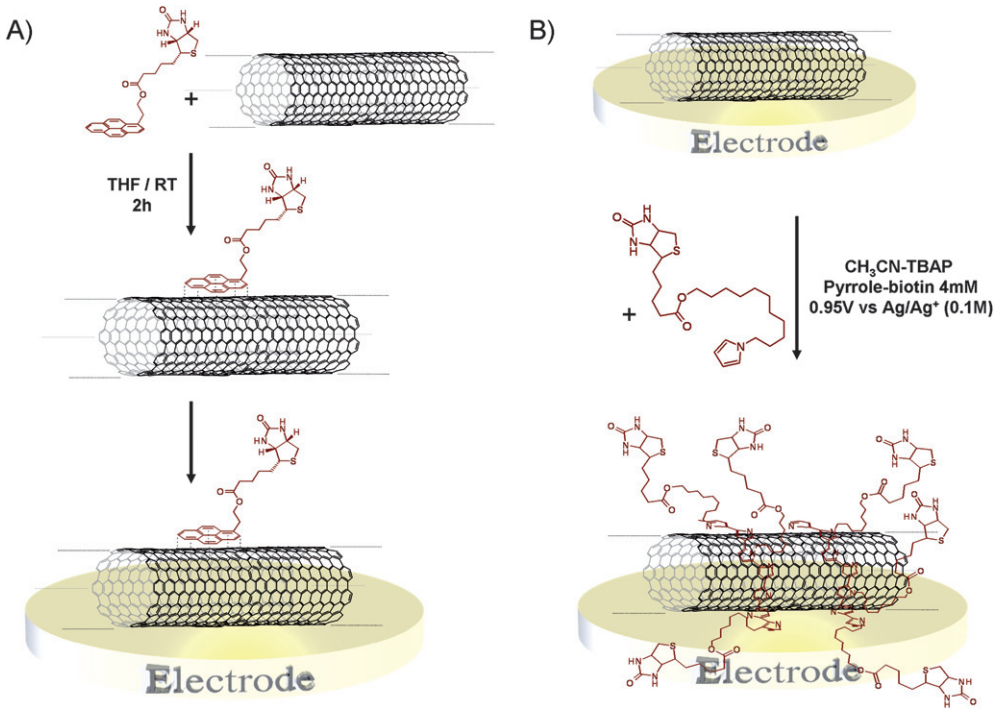

Scheme 1 Schematic presentation of the functionalization methods used for the attachment of biotin groups to the nanotubes. (A) Functionalization by π-stacking interaction between the pyrene–biotin derivative and the nanotube sidewalls and deposition of the biotinylated SWCNTs onto Pt-electrodes. (B) Electropolymerization of the pyrrole–biotin monomer on the SWCNTs, deposited on a Pt-electrode.

measurements and the amperometric response of these modified electrodes to glucose, which was oxidized into gluconic acid and H_2O_2. In addition, the effect of varying the amount of SWCNTs and/or enzyme layers on the performance of the resulting electrodes was also examined.

2. Results and discussion

2.1 Characterization using fluorescence microscopy

The effective immobilization of biotin groups on SWCNTs using electropolymerization or π-stacking interactions and its bioavailability for subsequent anchoring of avidin protein was investigated by fluorescence measurements with a streptavidin–phycoerythrin conjugate. The deposition of the carbon nanotubes was carried out on microelectrodes (10 μm diameter) arrayed on a silicon chip. The resulting modified biotin nanotube surfaces were exposed to a solution of streptavidin–phycoerythrin (0.5 mg mL^{-1}) over 20 min in darkness and then washed with stirred phosphate buffer solution (pH 7) and deionised water in order to avoid non-specific adsorption.

The efficient immobilization of phycoerythrin-labelled streptavidin on biotinylated polypyrrole films obtained by polymerization of pyrrole–biotin is demonstrated in Fig. 1B. For these experiments, three layers (each 4 μL) of the SWCNT dispersion were deposited on the electrode followed by the electropolymerization (0.1 mC) of a thin poly(pyrrole–biotin) film on the nanostructured surface. The same characterization was elaborated using a microelectrode covered by three layers of 4 μL of pyrene–biotin-modified SWCNTs.

The fluorescence depends on the presence of biotin at the surface of the microelectrodes. This indicates that the immobilization of the fluorescent streptavidin conjugate is specific for the avidin–biotin interaction. A cross-experiment based on bare microelectrodes (Fig. 1A) led to the absence of fluorescence, highlighting that the enzyme immobilization is due to the specific affinity interactions instead of non-specific adsorption.

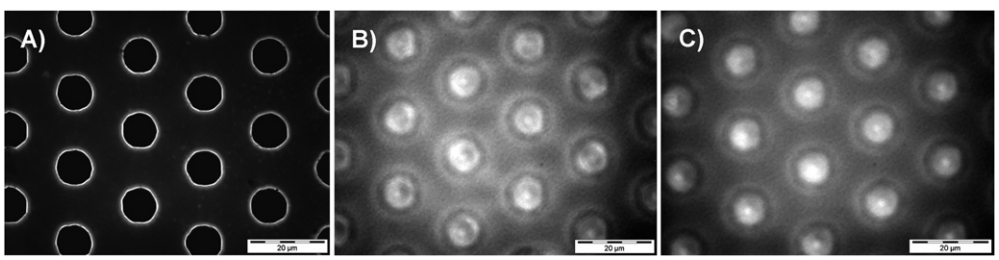

Fig. 1 Microelectrodes visualized by fluorescence microscopy after incubation with streptavidin–phycoerythrin: (A) bare electrode, (B) electrode covered with SWCNTs and a film of poly(pyrrole–biotin) and (C) electrode covered with pyrene–biotin SWCNTs.

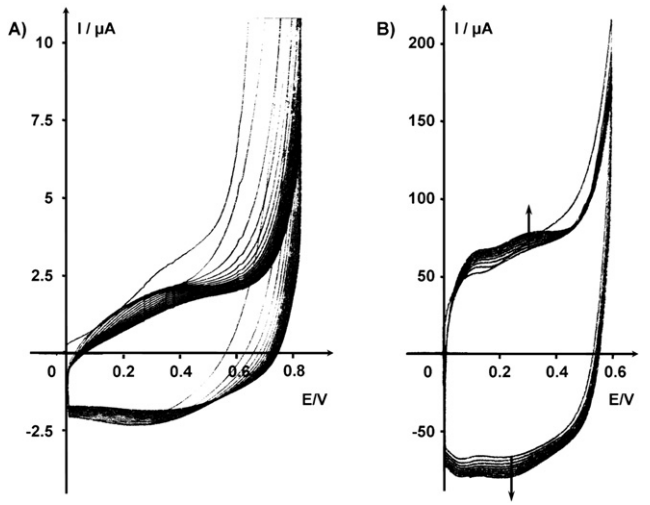

Fig. 2 Cyclic voltammogram of the oxidative polymerization of the biotin–pyrrole derivative on (A) a Pt-electrode by repeated potential scanning between 0 and 0.85 V, and (B) a SWCNT deposit (60 µL) on a Pt-electrode by repeated scanning between 0 and 0.6 V. Potentials were applied *versus* a 10 mM Ag^+/Ag in CH_3CN + TBAP (0.1 M) reference electrode; scan rate 100 mV s^{-1}.

It should be noted that the intensity of the fluorescence can be related to the amount of biotin derivative involved in the corresponding process. The streptavidin immobilization is more apparent in the case of the electropolymerization on the surface of the micro-spots while in the case of the SWCNT-pyrene–biotin sample (Fig. 1C) the fluorescence is less intense and the streptavidin is fixed even outside the micro-spots indicating the repartition of the modified carbon nanotubes on the whole surface of the microelectrode.

2.2 Characterization by cyclic voltammetry

The electrochemical behaviour of the poly(pyrrole–biotin) film in acetonitrile + 0.1 M TBAP was investigated by cyclic voltammetry. The cyclic voltammogram clearly shows an oxidation peak at 0.35 V and a reduction peak at 0.25 V due to the oxidation and reduction of the pyrrole group respectively. However, repeatedly scanning between 0 and 0.85 V shows no clear current intensity increases (Fig. 2A). This probably indicates the formation of an insulating polymer on the electrode surface as previously observed. To solve the problem of the conductivity of the pyrrole–biotin derivative, previous works were reported using a copolymer.[13,14]

The cyclic voltammograms of poly(pyrrole–biotin) electrogenerated on deposits of pristine nanotubes on a platinum electrode (60 µL and 80 µL) show oxidation waves at around 0.1 V and 0.3 V and reduction waves are observed at 0.05 V and 0.25 V. Repeated potential scanning of pyrrole–biotin over the range from 0 to 0.6 V results in the appearance and the continuous growth of the peak system for the reversible anodic and cathodic waves (Fig. 2B). As already observed for the electropolymerization of *N*-substituted pyrrole derivatives,[15] this clearly indicates the formation of an electrogenerated film on the nanostructured electrode surface.

2.3 Glucose response of the biosensor

The attachment of biotinylated glucose oxidase (B-GOX) on biotinylated SWCNTs *via* avidin bridges was investigated. The analytical characteristics of the constructed enzyme configuration towards the detection of the injected glucose were investigated by amperometry in 0.1 M phosphate buffer with an applied potential of 0.7 V. Under these conditions the enzymatically generated hydrogen peroxide is oxidized on the platinum electrode giving an electrochemical signal (current) which is directly correlated to the amount of generated H_2O_2.

Fig. 3 shows the anodic current response of the biosensors as a function of glucose concentration for different layers of pristine carbon nanotubes. The sensitivities of the SWCNT-based biosensors determined by the slope of the linear part of the calibration curve are 3.3, 5.2, and 1.3 mA M^{-1} cm^{-2} with a maximum current density of 22.5, 33.5, and 15 µA cm^{-2} for 40, 60, and 80 µL of the carbon nanotube deposits, respectively. Compared to the corresponding flat configuration of a polypyrrole film electropolymerized on a platinum electrode,[15,16] the high specific surface of SWCNTs for the 60 µL setup shows a more than ten-fold improvement of the glucose sensitivity due to the increased amount of anchored enzymes. In addition, a marked increase in maximum current density was observed. This suggests that the geometrical effect of the nanotube leads to a larger area covered by the poly(pyrrole–biotin) film and, therefore, increases in the amount of anchored GOX. It has to be noted that sensitivity and J_{max} clearly decrease for the sensor configuration corresponding to 80 µL of deposited SWCNT dispersion. This effect can be attributed to a more densely packed nanotube deposit and therefore to a diminished accessible surface and to the fact that the increased distance of the enzyme to the electrode provokes an increased loss of the enzymatically generated H_2O_2 in the bulk. This argument is supported by the clearly higher K_m value (4.8 mmol L^{-1}) of the setup with the highest amount of nanotubes (Fig. 3c) compared to the biosensors with 40 µL (2.7 mmol L^{-1}) and 60 µL (2.2 mmol L^{-1}) as seen

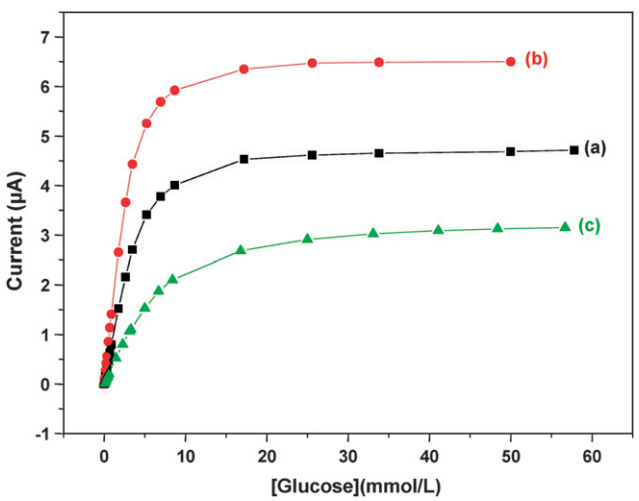

Fig. 3 Calibration curves of the glucose constructed on unmodified SWCNT deposit on Pt-electrodes using (a) 2 × 20 µL, (b) 3 × 20 µL, and (c) 4 × 20 µL of the SWCNT dispersion and a film of poly(pyrrole–biotin). Applied potential 0.7 V *versus* SCE; 0.1 M phosphate buffer (pH 7).

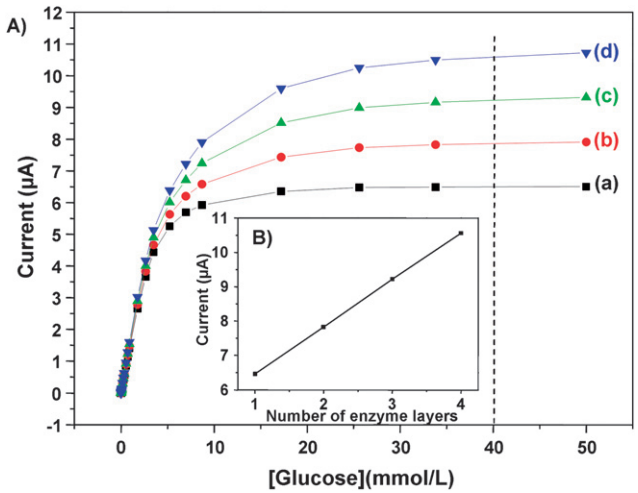

Fig. 4 (A) Calibration curves of the glucose constructed on unmodified SWCNT deposit on Pt-electrodes using 3 × 20 μL of the SWCNT dispersion and a film of poly(pyrrole–biotin) by successive incubations in (a) one, (b) two, (c) three and (d) four times in avidin and B-GOX. Inset (B) Evolution of the current *versus* the number of deposited avidin and B-GOX layers for 40 mM (see dashed line in part (A) of glucose concentration constructed on 60 μL of unmodified SWCNT deposit and a poly(pyrrole–biotin) film (0.54 mC).

in Fig. 3a and 3b, respectively. For the following experiments, all electrodes were prepared using 60 μL of the nanotube dispersion.

It has been reported that avidin–biotin interactions can successfully be used to build controlled molecular architectures composed of multienzyme layers.[7] Therefore, after optimisation of the amount of carbon nanotubes and the poly(pyrrole–biotin) thickness, the matrix has been applied for the construction of multienzyme layers by successive immersion of the modified electrode into an avidin and then into a B-GOX solution. Following this easy and fast procedure, several enzyme layers were fixed on the electrode surface. Fig. 4A shows the resulting calibration curves for glucose obtained with biosensors based on one, two, three, and four avidin/enzyme layers while Fig. 4B (inset) shows the evolution of the current *versus* the number of the avidin/B-GOX deposits for 40 mM of glucose concentration. As expected, the obtained results show a steady increase in maximum current density reflecting the higher amount of immobilized B-GOX. This evolution is linear, as shown for 40 mM of glucose (Fig. 4 inset).

Surprisingly, no evolution of the sensitivity for glucose can be observed. This can be due to a reduced permeability and hence a decrease in the H_2O_2 permeation through the polypyrrole-SWCNT film. The total coverage of the carbon nanotube film by the polymer generates constraints towards the diffusion of H_2O_2 through the polymer and therefore inhibits the increase of sensitivity.

Our second approach consisted of the deposition of biotin–pyrene-functionalized SWCNTs on the Pt-electrodes to allow the formation of an avidin monolayer and, thus, the anchoring of B-GOX over the whole accessible surface. Fig. 5 represents the resulting biosensor responses as a function of glucose concentration for different layers of deposited pyrene–biotin SWCNTs. All sensitivities were determined by the slope of the linear part of the calibration curve. The glucose sensitivity for such modified electrodes increases linearly with increasing amount of deposited pyrene–biotin SWCNTs. For 40 μL of the pyrene–biotin SWCNT dispersion, a sensitivity of 0.35 mA M^{-1} cm^{-2} was obtained. For 60 μL and 80 μL of the deposited pyrene–biotin SWCNT dispersion, 0.56 mA M^{-1} cm^{-2} and 0.77 mA M^{-1} cm^{-2} were measured. The comparison with the sensitivities of the corresponding polypyrrole configuration with an increasing amount of pristine carbon nanotubes highlights the beneficial role played by the absence of the polymer film despite the estimated higher hydrophobic character of the pyrene–biotin-functionalized nanotubes. The immobilization of different layers of avidin and B-GOX onto pyrene–biotin SWCNTs led to an increase in both the sensitivity and maximum current density. These results indicate an unhindered permeation of H_2O_2. Fig. 6A, 6B and 6C show the obtained calibration curves for glucose sensors with different avidin/enzyme layers, each immobilized on deposits of 40, 60, and 80 μL of the pyrene–biotin SWCNT dispersion. This demonstrates the reproducible elaboration of nanotube and enzyme layers where the maximum current at saturating glucose concentrations is related to the amount of immobilized B-GOX. Moreover, the evolution of the current *versus* the number of avidin and B-GOX deposits is linear as shown in Fig. 6D for 40 mM of glucose and for different pyrene–biotin SWCNT deposits. This linear evolution for the different enzyme layers indicates the successful elaboration of three-dimensional architectures. Moreover, the progress of the slope with the modified SWCNT layers is in a good correlation with the amount of adsorbed nanotubes on the electrode surface showing the excellent control of the nanotube deposits. Since the maximum current density reflects the amount of immobilized enzymes to be independent to permeability effects, we can conclude our results for our biosensors using differently modified nanotubes by comparing the J_{max} values of both setups. Regarding the same amount of deposited nanotubes (60 μL) with 4 enzyme layers (see Fig. 4A(d) and Fig. 6B(d)), the biosensor using the polypyrrole-modified SWCNT deposit shows 55 μA cm^{-2} while for the biotin–pyrene-functionalized nanotubes 34 μA cm^{-2} could be reached. The distribution of biotin groups

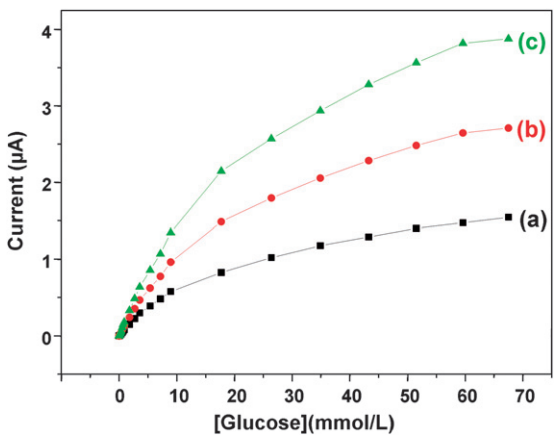

Fig. 5 Calibration curves for biotinylated SWCNT deposits constructed by π-staking on Pt-electrodes using (a) 40 μL, (b) 60 μL, and (c) 80 μL of the pyrene–biotin SWCNT dispersion deposited on Pt-electrodes followed by functionalization with avidin and B-GOX.

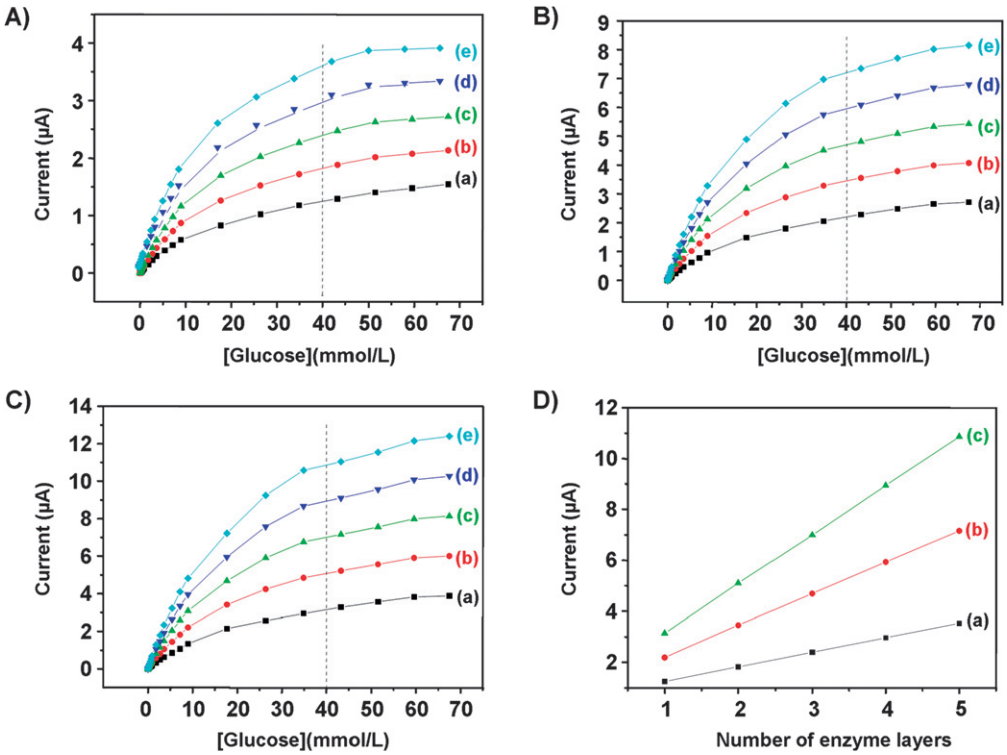

Fig. 6 (A) Steady state current responses of the biosensor constructed on pyrene–biotin SWCNTs to glucose increments using 2 × 20 μL of the modified-SWCNT electrode which has further been treated by successive incubations of (a) one, (b) two, (c) three, (d) four, and (e) five times in solutions of 0.5 mg mL^{-1} of avidin and B-GOX. (B) Steady state current responses of the biosensor constructed on biotin–pyrene-modified CNT to glucose increments using 3 × 20 μL of the modified-SWCNT electrode which has further been treated by successive incubations of (a) one, (b) two, (c) three, (d) four, and (e) five times in solutions of 0.5 mg mL^{-1} of avidin and B-GOX. (C) Steady state current responses of the biosensor constructed on pyrene–biotin SWCNTs to glucose increments using 4 × 20 μL of the modified-SWCNT electrode which has further been treated by successive incubations of (a) one, (b) two, (c) three, (d) four, and (e) five times in solutions of 0.5 mg mL^{-1} of avidin and B-GOX. (D) Evolution of the current *versus* the number of deposited layers of avidin and B-GOX for 40 mM of glucose concentration (see dashed lines in 6A–C) constructed on (a) 2 × 20 μL, (b) 3 × 20 μL, and (c) 4 × 20 μL of pyrene–biotin SWCNTs.

on the biotin–pyrene-functionalized nanotube sidewalls is less pronounced than for the polypyrrole film which explains the inferior amount (0.63 equiv.) of immobilized enzymes. Against this, increasing the amount of biotin–pyrene-functionalized nanotubes shows no restrictions in permeability. Constructing the biosensor by depositing 80 μL of the biotin SWCNT dispersion almost the same J_{max} value (53 μA cm^{-2}) as for the poly(pyrrole–biotin) configuration could be obtained after 4 enzyme layers (Fig. 6C(d)). For the 5th enzyme layer as shown in Fig. 6C(d), this setup even surpassed the J_{max} value (65 μA cm^{-2}) of the poly(pyrrole–biotin) equivalent reflecting the high potential of such nanotube derivatives for biosensor application.

3. Experimental

3.1 Reagents

Avidin and biotin-labelled glucose oxidase (GOX, 120 U mg^{-1}) were purchased from Sigma while tetra-n-butyl ammonium perchlorate (TBAP) was purchased from Fluka and was recrystallized from ethyl acetate and cyclohexane and dried under vacuum at 80 °C for 3 days. Streptavidin–phycoerythrin conjugate was purchased from Molecular Probes. All other chemicals were obtained commercially and were of analytical grade. Glucose solutions were allowed to mutarotate at room temperature for 24 h before use and were kept refrigerated.

Single-walled carbon nanotubes, produced by the HiPco® process (Purified, CNI grade/Lot #: P0313), were purchased from Carbon Nanotechnologies, Inc. (CNI). To obtain better dispersions, as received HiPco® nanotubes (20 mg) were dispersed in 300 mL of THF in an ultrasonic bath for three hours. The solvent of the inhomogeneous dispersion was then evaporated in a vacuum to recover a fine powder of carbon nanotubes. The solid was diluted with 200 mL DMF and sonicated for a further two hours at room temperature. After sedimentation of undispersed nanotubes, the supernatant was filtered over a PTFE membrane filter (pore size: 0.45 μm) and washed with THF. The residue was not allowed to dry during filtration. Thus, the wet sludge cake was put in a few millilitres of diethyl ether and mechanically stirred and ground until dryness to avoid re-aggregation of the SWCNTs. Using such pre-treated nanotubes, stable and homogeneous dispersions in THF can be obtained after only 20–30 min of sonication.

Pyrrole–biotin ester,[15] pyrenebutanol biotin ester and biotinylated SWCNTs[17] were synthesized as described with slight modifications.

Biotin–pyrenebutyl ester: pyrenebutanol (280 mg, 1.0 mmol) was dissolved in 20 mL DMF under an argon atmosphere. The

coupling reagents (DCC, 280 mg, 1.35 mmol; DMAP, 100 mg, 4.2 mmol) were added to this solution as well as biotin (0.250 g, 1.0 mmol). The reaction was observed by TLC (solvents: CH_2Cl_2/EtOH 95:5; retention 0.5). After one week of reaction time, the solvent was evaporated and the yellow solid was dissolved in CH_2Cl_2. Biotin–pyrene was purified by flash chromatography (mobile phase CH_2Cl_2/EtOH 95:5) on silica gel 60 μm particle size as the stationary phase. ^{1}H NMR ($CDCl_3$, 250 MHz): δ ppm = 8.23 (1H, d), 8.07 (7H, m), 7.85 (1H, d), 5.52 (1H, s), 5.12 (1H, s), 4.25 (1H, t), 4.12 (2H, t), 4.05 (1H, d), 3.35 (2H, t), 2.92 (1H, d), 2.72 (2H, 2×dd), 2.27 (2H, t), 1.90–1.23 (10H, m). MS (EI, 200 °C): m/z = 503 (MH^+, $C_{30}H_{34}N_2O_3S$).

11-Biotin-(1-pyrrolyl)undecyl ester: biotin (500 mg, 2 mmol), 11-(1- pyrrolyl)undecanol (208 mg, 1.66 mmol), DCC (413 mg, 2 mmol) and DMAP (81 mg, 0.66 mmol) were dissolved in dry CH_2Cl_2. The mixture was stirred under argon for 6 days at room temperature and then filtered. The organic phase was evaporated and the residue was washed with Et_2O. The resulting product was purified by flash chromatography on silica gel with CH_2Cl_2/EtOH (95:5). Crystallization from CH_2Cl_2/Et_2O gave the pure product. MS (EI, 200 °C): m/z = 464 (MH^+, $C_{25}H_{41}N_3O_3S$). ^{1}H NMR (DMSO-d_6, 200 MHz) δ ppm = 1.14–1.5 (m, 10H), 1.75 (m, 14H), 2.04 (t, 2H), 2.68 (m, 1H), 2.86 (m, 1H), 3.08 (m, 1H), 4 (m, 4H), 4.26 (m, 1H), 4.46 (m, 1H), 5.61 (s, 1H), 6.04 (s, 1H), 6.14 (m, 2H), 6.64 (m, 2H).

For the SWCNT functionalization by π-stacking interactions, pre-treated HiPco® nanotubes (20 mg) were dispersed in 150 mL THF. After sedimentation of not-dispersed nanotubes, the dark but still transparent dispersion was decanted off and 20 mg (40 μmol) of pyrenebutanol biotin ester was added. After 3 h of stirring at room temperature, the non-covalently functionalized nanotubes started to precipitate. The supernatant was decanted off and the sediment was diluted with THF and sonicated for 1 h. The product was filtered over a PTFE membrane filter (pore size: 0.45 μm) and washed with DMF, THF and CH_2Cl_2 to remove the excess of the pyrene–biotin derivative.

3.2 Measurements and apparatus

All electrochemical measurements were performed with a conventional three-electrode system. A saturated calomel electrode (SCE) and a Pt wire placed in a separate compartment containing the aqueous electrolyte were used as reference and counter electrode, respectively. The working electrode was a platinum disk electrode with 5 mm diameter, polished with 2 μm diamond paste (MECAPREX Press PM) followed by rinsing with distilled water, ethanol and acetone. The amperometric measurements were carried out with a Tacussel PRG-DL potentiostat in phosphate buffer solution (PBS, 0.1 M, pH 7) in a thermostated cell at 25 °C under stirred conditions. Cyclic voltammetry experiments were performed with an EGC PARC, Model 173 potentiostat equipped with a Model 175 universal programmer and a Model 179 digital coulometer in conjunction with a Serfam TGM 164 XY/t recorder.

Substrates were visualized by fluorescence microscopy (Olympus BX61) at 488 nm excitation and 578 nm emission wavelengths equipped with a DCC camera using microelectrodes.

3.3 Preparation of the electrodes

In order to design new biological 3D architectures based on SWCNTs, we have first functionalized SWCNT coatings by a poly(pyrrole–biotin) film. The SWCNT layers were formed after deposition of 20 μL of the SWCNT–THF dispersion on Pt-electrodes (∅ 5mm) followed by evaporation of the solvent in a vacuum. These steps were repeated to obtain 40 μL, 60 μL and 80 μL coatings of the pristine carbon nanotubes. Since the SWCNT concentrations of the THF dispersion can only be approximately estimated (around 0.01 mg mL^{-1}), the layers will further be denoted with the used quantities (μL) of the deposited dispersion. The homogeneity of the deposits was evaluated by optical microscopy. Only deposits where no large aggregates were visible were used for our experiments. Due to the pre-treatment, no surfactants or additives were necessary to obtain homogeneous dispersions. Therefore, stable deposits could be formed on the electrodes. The electrochemical polymerization of pyrrole–biotin onto the deposits was performed in CH_3CN + 0.1 M TBAP containing biotin–pyrrole (4 mM) at a constant potential (0.95 V) in a glove box under an argon atmosphere. All nanotube deposits were evaluated with scanning electron microscopy and compared to precedent experiments.[17,18] These modified electrodes were then incubated in 20 μL of avidin solution (0.5 mg mL^{-1}) for 20 min. The resulting electrodes were carefully washed with PBS (0.1 M, pH 7.0) and 20 μL of B-GOX (1 mg mL^{-1} in PBS) was deposited on the electrode surfaces and left for 20 min at 4 °C. The resulting enzyme electrodes were thoroughly rinsed in PBS (0.1 M, pH 7.0) before being used for the amperometric measurements.

The preparation of the electrochemical sensor modified using dispersions of biotin–pyrene-functionalized SWCNTs consists of, as described above, casting the platinum electrode (∅ 5 mm) with successive drops of 20 μL followed by drying in a vacuum in order to obtain different layers of biotin-modified carbon nanotubes formed with 40 μL, 60 μL and 80 μL from the given THF dispersions. Avidin and B-GOX were immobilized on the biotinylated SWCNT-modified electrodes, as previously described, for the poly(pyrrole–biotin)-modified SWCNT electrode.

4. Conclusion

Among the numerous procedures of protein immobilization, carbon nanotubes have been demonstrated to be an excellent material for the development of electrochemical sensors.

The electropolymerization of pyrrole–biotin monomers onto a deposit of single-walled carbon nanotubes combined with the avidin–biotin affinity interactions offered large potentiality for biosensor construction and the control of the electrochemical characteristics of the bioelectrodes. Moreover, the successive anchoring of avidin and enzyme molecules constitutes an attractive way for the elaboration of multilayered enzyme immobilization. However, a reduced permeability of hydrogen peroxide through the polymer film can be seen as a limiting factor for this biosensor setup. Against this, deposits of non-covalent functionalization using π-stacking interactions between pyrene–biotin and carbon nanotubes offers an optimal diffusion of H_2O_2, even at high amounts of deposited SWCNTs and enzyme layers. Therefore, such biotinylated SWCNTs have a more

promising potential for the fabrication of biosensors. Fluorescence microscopy studies allowed the determination of the avidin–biotin affinity and demonstrated the reliability of this anchoring method on modified electrode surfaces.

The unique properties of nanotubes for the enhancement of the accessible surface area contribute in a large extent to the design of a new generation of biosensors with high analytical performances able to address future challenges in clinical diagnostics, environmental monitoring and security control.

Acknowledgements

The authors would like to thank the MIRA cooperation program of the Rhone Alpes region, France, for their partial financial support of this work. We also would like to acknowledge the platform 'functionalization of surfaces and transduction' of the scientific structure 'Nanobio' for providing facilities. Arielle LePellec is greatly acknowledged for technical assistance.

References

1 S. J. Updike, B. J. Gilligan, M. C. Shults and R. K. Rhodes, *Diabetes Care*, 2000, **23**, 208–214.
2 R. Lenigk, E. Lam, A. Lai, H. Wang, Y. Han, P. Carlier and R. Renneberg, *Biosens. Bioelectron.*, 2000, **15**, 541–547.
3 K. Rekha, M. D. Gouda, M. S. Thakur and N. G. Karanth, *Biosens. Bioelectron.*, 2000, **15**, 499–502.
4 B. Adhikari and S. Majumdar, *Prog. Polym. Sci.*, 2004, **29**, 699–766.
5 L. Coche-Guérente, S. Cosnier, C. Innocent and P. Mailley, *Anal. Chim. Acta*, 1995, **311**, 23–30.
6 J.-i. Anzai, Y. Kobayashi, Y. Suzuki, H. Takeshita, Q. Chen, T. Osa, T. Hoshi and X.-y. Du, *Sens. Actuators, B*, 1998, **52**, 3–9.
7 S. Cosnier, C. Gondran, A. L. Pellec and A. Senillou, *Anal. Lett.*, 2001, **34**, 61–70.
8 H.-L. Hsu and J.-M. Jehng, *Mater. Sci. Eng., C*, 2009, **29**, 55–61.
9 H. N. Choi, Y.-K. Lyu, J. H. Han and W.-Y. Lee, *Electroanalysis*, 2007, **19**, 1524–1530.
10 A. Callegari, S. Cosnier, M. Marcaccio, D. Paolucci, F. Paolucci, V. Georgakilas, N. Tagmatarchis, E. Vázquez and M. Prato, *J. Mater. Chem.*, 2004, **14**, 807–810.
11 A. Arvinte, A. M. Sesay, V. Virtanen and C. Bala, *Electroanalysis*, 2008, **20**, 2355–2362.
12 J. J. Davis, K. S. Coleman, B. R. Azamian, C. B. Bagshaw and M. L. H. Green, *Chem.–Eur. J.*, 2003, **9**, 3732–3739.
13 S. Cosnier and A. Lepellec, *Electrochim. Acta*, 1999, **44**, 1833–1836.
14 R. E. Ionescu, C. Gondran, L. A. Gheber, S. Cosnier and R. S. Marks, *Anal. Chem.*, 2004, **76**, 6808–6813.
15 S. Cosnier, B. Galland, C. Gondran and A. L. Pellec, *Electroanalysis*, 1998, **10**, 808–813.
16 S. Cosnier, M. Stoytcheva, A. Senillou, H. Perrot, R. P. M. Furriel and F. A. Leone, *Anal. Chem.*, 1999, **71**, 3692–3697.
17 M. Holzinger, R. Haddad, A. Maaref and S. Cosnier, *J. Nanosci. Nanotechnol.*, 2009, **9**, 6042–6046.
18 M. Holzinger, L. Bouffier, R. Villalonga and S. Cosnier, *Biosens. Bioelectron.*, 2009, **24**, 1128–1134.

